

# Mechanisms in creep and hot working to high strain; microstructural evidence, inconsistencies.

## Part I: substructure evolution; grain interactions

H.J. McQueen, Mech., Ind. Engr., Concordia University, Montreal - Canada

Distinguished Research Professor, Dept. Chemical and Materials Engineering, University of Dayton, OH (USA)

### ABSTRACT

*The dislocation mechanisms of dynamic recovery (DRV) in metals of high stacking fault energy (SFE) give rise to steady-state straining dependent on temperature and strain rate due to development of constancy in the spacings of subgrain boundaries ( $w_S$ , SGB) and of the dislocations within both the SGB and the subgrains. When the grains are large compared to subgrains, the interactions of grain boundaries with SGB are limited to serration formation but when one-grain dimension is reduced to about twice the SGB spacing, the interactions begin to define a minimum grain dimension. However, the cellular size defined by the mixture of SGB and GB remains constant at  $w_S$  along with the stress. In metals of low SFE, the above is seldom attained since dynamic recrystallization (DRX) intervenes to provide new grains more than twice the subgrain size. On a larger scale, transition boundaries between deformation bands lying between differently slipping and rotating bands, become permanent and rapidly rise in angle and take on GB behavior in both DRV (serrations) and in DRX (nucleation sites). The evidence became more precise as techniques advanced through polarized optical, scanning and transmission electron and orientation imaging microscopies; however, deficiencies in each technique often created confusions that were resolved only through detailed comparison of the evidence.*

### RIASSUNTO

Il rinvenimento dinamico (DRV) nei metalli che hanno elevata energia del difetto di impilaggio (SFE) coinvolge meccanismi di riassetto delle dislocazioni che danno luogo allo stato stazionario della tensione il cui valore è funzione della  $T$  e della velocità di deformazione. Questo è dovuto alla formazione di sottogranì a grandezza costante e di dislocazioni all'interno sia dei sottogranì che del loro confine ( $w_S$ , SGB). Essendo i grani grandi rispetto ai sottogranì, le interazioni del confine di grano (GB) con SGB è limitata alla formazione della dentellatura che riduce la dimensione del grano a circa il doppio della spaziatura del SGB; le interazioni portano a definire una dimensione minima del grano. La grandezza delle celle, definita dalla interazione tra SGB e GB, resta costante a  $w_S$  assieme alla tensione. Nei metalli a bassa SFE il comportamento descritto si verifica raramente in quanto per effetto della ricristallizzazione dinamica (DRX) si formano grani nuovi, grandi più del doppio dei sottogranì. Su scala più ampia, i confini di transizione tra le bande di deformazione, che sono comprese tra quelle di scorrimento e quelle di rotazione, diventano stabili, aumentano rapidamente di angolo e assumono il comportamento del GB sia nel DRV (dentellatura) che nella DRX (siti di nucleazione). La conoscenza dei fenomeni esposti è diventata più esatta con il progresso delle tecniche di indagine quali la microscopia a luce polarizzata, la microscopia elettronica a scansione, in trasmissione e ad orientazione di immagine. Spesso i limiti inerenti a ciascuna tecnica hanno creato confusioni che sono state risolte solo attraverso il confronto dettagliato delle immagini.

### KEYWORDS

*Hot working, dynamic recovery, transition boundaries, grain defining gDRV, dynamic recrystallization.*

### NOTA/REMARK

*The II Part will be included at Metallurgical Science and Technology Vol. 28-2.*

## INTRODUCTION

The objective is to describe for three distinct control factors the microstructural evolution feature by feature at distinctive stages up to high strains  $\varepsilon$  in steady state for hot working and creep. The high degree of dynamic recovery (DRV) causing subgrain boundaries (SGB) is described for aluminum and ferritic alloys with high stacking fault energy (SFE) [1-8]. However, deformation bands with transition boundaries are controlled by plastic stability and serrations in grain boundaries (GB) by surface energy. As clarification by contrast, substructures in low SFE metals (Cu, Ni, austenitic  $\gamma$ -Fe) give rise to dynamic recrystallization (DRX) including

discontinuous dDRX [1-7,9], continuous cDRX and particle stimulated nucleation PSN-DRX. For simplicity, the lower limit for elevated temperature  $T$  is about half the melting point ( $T_M$ , K). To enhance permissible strain (ductility  $\varepsilon_F$ ) in hot working,  $T$  is usually higher than in creep where the objective is to reduce the strain rate ( $\dot{\varepsilon}$ ). In hot working tests,  $\dot{\varepsilon}$  is usually constant whereas in creep tests it is the stress  $\sigma$ . In real processing or applications  $T$ ,  $\varepsilon$ ,  $\dot{\varepsilon}$ ,  $\sigma$  are varying in time and possibly in space. The extensive experimental evidence is not described but references are provided to both varied original experimental evidence and to reviews.

In the second part of the paper, the evidence is presented by experimental technique in roughly historical order of development; the objectives there are to clarify the theories developed and the problems that arose due to limitations of the techniques. The constitutive evidence is given minor coverage since it generally confirms the mechanisms as DRV [10,11]. The activation energy  $Q$  shifts to higher values when there are peaks before the steady state as a result of either discontinuous dDRX. It rises above that for self diffusion as there are increased obstacles to dislocation motion as has been detailed in previous reviews.

## DYNAMIC RECOVERY PHENOMENA: {-DRV}

The microstructural evolution is divided into sections to distinguish phenomena, the present one being {-DRV}; these are subdivided to emphasize certain mechanisms. In each section explanations progress from the well established to the more advanced. The terminology employed is drawn from papers explaining standardization of strain-induced boundaries (SIB) [12,13].

**1-DRV.** In hot strain hardening (primary creep), the dislocations leave their slip planes easily in wavy glide and progress into tangles and SGB formation; this is noted as a slope change in  $\theta$ - $\sigma$  plots ( $\theta = d\sigma/d\varepsilon$ ). This entire stage is referred to as the transient strain and is marked by  $\theta$  declining in fairly linear segments to zero. In some solute alloys notably Al-Mg, different behavior is described later [14, 15]. Such polygonization is also found as a function of time in static recovery (SRV) but at a much lower, declining rate as driven by substructure stress fields whereas DRV is driven by constant applied  $\sigma$  or  $\dot{\varepsilon}$  [5, 17-21]. For equivalent homologous conditions ( $T/T_M$  melting  $T$ ), alloys of Ni,  $\gamma$ -Fe and Cu are polygonized to a lower degree as SFE declines [1, 6, 9, 15, 17].

**2-DRV.** With formation of a fairly uniform subgrain structure of diameter  $d_s$  ( $0.787 d_s = w_s$  wall spacing) steady state straining proceeds at constant stress  $\sigma_s$  with the relationships at right side (Figures 1 [149],

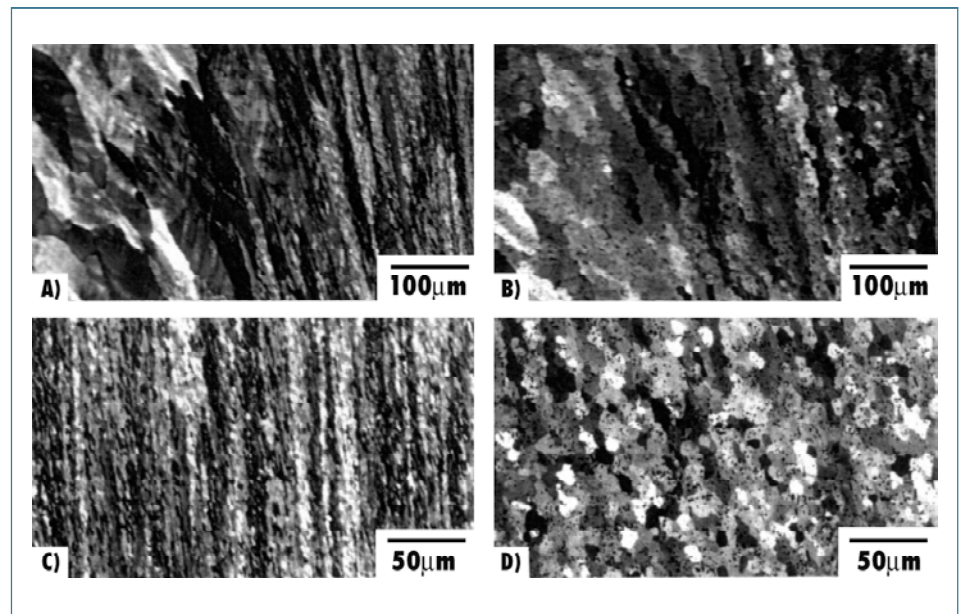


Fig. 1: Polarized optical microscopy of Al-0.9Mn (fine  $Al_3Mn$  dispersoid) after torsion to  $\varepsilon = 12$  at  $1 s^{-1}$  with (a, b) showing transition from shoulder to gage (right) and (c, d) gage at twice magnification: a, c) 400°C and b, d) 500°C (DB in grain just above (b)).

2 [57, 91, 150]). Equations 1 and 2 are independent of  $\varepsilon$  in steady state [3, 5, 7, 11, 16, 18, 23-27]. (Eq. 2 applies to yield at 20 °C [28,29]:

$$d_s^{-1} = a + b \log \{ \varepsilon \exp (Q_{HW}/RT) \} = a + b \log Z \quad (1)$$

$$\sigma_s = c + e d_s^{-p} \quad (2)$$

$$fn(\sigma_s) = \dot{\varepsilon} \exp (Q_{HW}/RT) \quad (3)$$

$$\text{Where } fn(\sigma_s) \text{ may be } A (\sinh \alpha \sigma_s^n), \text{ or } A' \sigma_s^{n'}, \text{ or } A'' \exp (\beta \sigma_s) \quad (4)$$

with material constants  $a, b, c, e, A, A', A'', n, n'$  (stress exponents),  $\alpha, \beta$  (stress multipliers),  $p$  approximately 1,  $Q_{HW}$  for hot working and  $Q_{CR}$  for creep, and  $R$  gas constant [3, 4, 10, 11, 16, 23, 24, 27]. The Zener-Hollomon parameter  $Z$  includes the two control parameters  $T, \dot{\epsilon}$  in hot working. The sinh law spans the stresses in hot working whereas the power law is well accepted for creep and the exponential for high stress. These equations also apply to low SFE metals and alloys better at higher  $T/T_M$  and in creep [3, 10, 15, 23].

**3-DRV.** While the constancy of  $d_s$  or  $w_s$  is relatively well accepted, it is related to both the dislocation spacing  $(\rho_i)^{0.5}$  in the Frank network inside the subgrains and  $S_w$  in the walls. In creep analysis,  $\rho_i$  is frequently considered to provide rate control of dislocation migration ( $\dot{\epsilon}_s$ ) for a given  $\sigma$  and  $T_D$  ( $T$  deformation) [12, 13, 23, 30-37]. This contrasts with cold working where flow stress is thought to depend primarily on spacing in the dislocation walls (11-DRV) [38].

**4-DRV.** The SGB misorientation  $\Psi (=b/S_w)$  ( $S_w$  dislocation density in the walls) has been measured over a wide range of strains [30-35, 38-41] and most notably in a project to  $\epsilon = 16$  [41]; these extensive results indicate that  $\Psi$  is constant. However, there is a dispute at high strains ( $\epsilon > 20$ ) that  $\Psi$  increases that is related to differing experimental interpretation (4, 6-SERV; 13, 14, 15-DRX) (Part II). Constancy of  $\Psi$  is related to repolygonization (7-DRV).

**5-DRV.** The values of  $w_s, (\rho_i)^{0.5}$  and  $\Psi_s$  for a given condition  $T, \dot{\epsilon}, \sigma_s$  are called the characteristic values [30-37, 42]. Log-log plots of these values against  $\sigma_s/G$  ( $G, \sigma_s$  shear modulus) for similar alloys are linear. The normalized creep rate is also a function of  $\sigma/G$ .

$$\epsilon_s k_B T / DGb = f_n (\sigma_s / G) \quad (5)$$

where  $k_B$  is Boltzman constant,  $D (=D_0 \exp(-Q_D/RT), Q_D$  for self diffusion),  $b$  Burgers vector. The consistency of these relationships for both spacings and  $\epsilon$  have been confirmed in one project for Al, Al-11Zn, Al-5Mg, Al-5Mg-Mn [14, 34, 35] for a wide range of  $\epsilon$  in creep and in hot torsion. The consistent relationship of these microstructural features and  $\epsilon_s$  to  $\sigma_s$

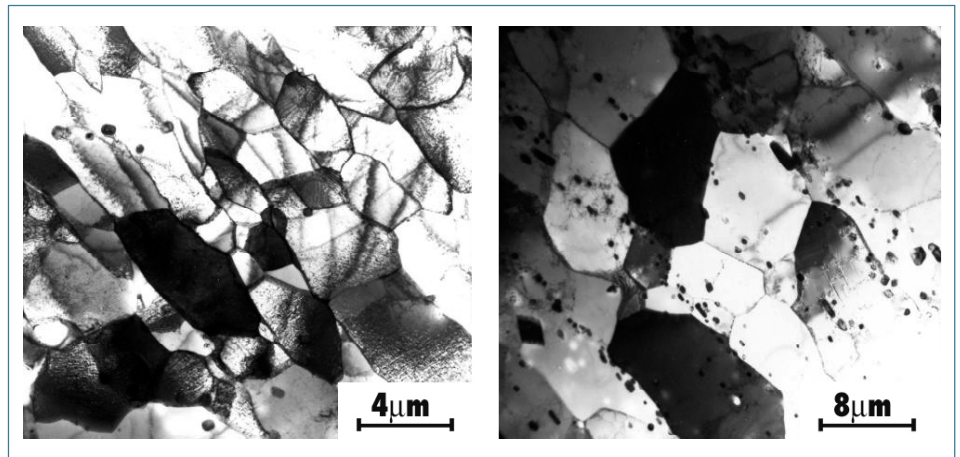


Fig. 2: Transmission electron microscopy of Al-0.65Fe after torsion to  $\epsilon = 0.3$  at 400°C: a) 1 s<sup>-1</sup>, elongated subgrains, Al<sub>3</sub>Fe in SGB and b) 0.1 s<sup>-1</sup>, subgrains twice size containing Al<sub>3</sub>Fe (fractured eutectic rods) with some Orowan loops in contrast.

indicates that the stress fields of any one stabilize the others so that all together are rate controlling as expressed in creep.

**6-DRV.** The stress field around SGB has been found asymmetric indicating the presence of a forward residual stress ( $\sim 0.5\sigma$ ) that assists the release (or passage through) of dislocations [30-35, 43]. Within the subgrains there is a back stress ( $\sim 5\sigma$ ) that slows passage through the Frank network; nevertheless in pure Al, they literally fly across [44-47].

**7-DRV.** With rising strain, the subgrains remain equiaxed inside elongating grains. Evidently the SGB continually rearrange (repolygonization) by decomposing (unknitting), forming (reknitting), migrating and merging (raising  $\Psi$  temporarily) or annihilating. SGB are clearly transitory [4, 19, 34, 39, 44-46, 48-50].

**8-DRV.** When during steady state 1 ( $\sigma_s, \epsilon_{s1}, T_1, d_{s1}, w_{s1}, \rho_{i1}, S_{w1}$ ), a change  $\Delta\dot{\epsilon}$  (or  $\Delta\sigma$  in creep) possibly instantaneous or  $\Delta T$  causes a gradual change to characteristic substructure of the new steady state. This is a controlled repolygonization that requires larger time or  $\Delta\epsilon$  as  $\Delta\dot{\epsilon}$  (or  $\Delta\sigma$ ) are larger; this is consistent with the dependence of initial transient on  $\dot{\epsilon}$  or  $\sigma$  [37, 45, 46, 51-54]. Accordingly as postulated for a given straining condition, the continual repolygonization (in 7-DRV) is completed every strain interval equaling the initial transient [12, 13, 32, 33].

**9-DRV.** Al-Mg alloys exhibit an inverted transient compared to Al (1-DRV) in so far

as a high stress is required to move dislocations away from Cottrell solute atmospheres and then declines as the mobile dislocations density increases [14, 34, 35, 40, 55, 56]. The dislocations first organize into layers and only gradually cross linking occurs to form subgrains to reach a substructural steady state  $\epsilon_{ss}$  some 50% higher than the mechanical  $\epsilon_{SM}$  [35, 55]. At the same  $\sigma_s/G$  the subgrains dimensions (5-DRV) are about the same as in Al, whereas at the same  $Z$  ( $T, \dot{\epsilon}$ ) they are about 1/4 to 1/5 the size.

**10-DRV.** As a result of solute drag, most effective near 5% Mg, the exponent in the power law (2-DRV) or normalized form (5-DRV) is close to 3 instead of 5 over a limited domain in which the solute atoms diffuse rapidly enough to cling along the dislocations [14, 34, 35, 55, 57]. In reference to the composite theory (6-DRV), the forward stress at SGB is much less and in the subgrain interior back or friction stress is much greater so dislocations move sedately due to viscous drag.

**11-DRV.** Because in Al and  $\alpha$  Fe there is a continuous rise in flow curves with decreasing  $T$ , there must be a continuous alteration in the repolygonization of SGB from that characteristic of DRV in hot working to that for cold working with rising intensification of  $\Psi$  [11-13, 55, 56, 58]. This continual rise in  $\Psi$  takes place in block walls (BW, also called Geometrically Necessary Boundaries, GNB) that form a network ( $\sim 5\mu m$ ) enclosing an array of cell

walls ( $\sim 0.5\mu\text{m}$ ) that are transitory [30-33, 38, 59-63]. As  $T$  declines, the unknitting and rearranging mechanisms become less effective so that there is a growing number of regions with high  $\Psi$  cell walls. This also occurs in  $\alpha$  matrix constrained by  $\gamma$ -phase

in duplex stainless [66]. This phenomenon, possibly called warm w-DRV, is progressing towards Stage III DRV noted in single-slip crystals. The continual rise in  $\Psi$  of most block walls (GNB) to exceed  $30^\circ$  is considered to be the major cause of

continued strain hardening [64, 65]; their spacing is similar to that of SGB. The cell walls, that are transitory like SGB, have a spacing of only  $0.5\mu\text{m}$  with slow rise in  $\Psi$  [12, 13].

## DEFORMATION BANDS - TRANSITION BOUNDARIES (TB): {-DBTB}

**1-DBTB.** Deformation bands refer to regions of a crystal or grain that are slipping on different systems. The dislocations from both regions interact to form a transition boundary (TB) that rises rapidly in  $\Psi$  [21, 31, 67-74]. This is associated with the regions rotating differently (approximately slip direction into elongation axis). Moreover, these boundaries are essentially permanent passing through the sequence low (LAB  $0-5^\circ$ ) and medium (MAB  $6-14^\circ$ ) to high angle (HAB  $> 15^\circ$ ). Evidence from cold working and from single crystals is described to clarify hot working behavior. In difference from these, are shear bands that occur at  $40^\circ\text{C}$  to the rolling direction in some grains with slip planes so oriented in the plane of maximum shear stress; in repeated passes they occur in new grains that have rotated [75]; permanent shear bands crossing GB were observed in cyclic-extrusion-compression [76].

**2-DBTB.** In single crystals at  $20^\circ\text{C}$  with single slip studied by successive surface markings, a kink running across slip bands initiates at a stress disturbance resulting from particles, mosaic walls or bending [70]. The kink widens developing between two TB an interior with slip on a new system or multiple slip with the old one. TEM of a well-developed TB shows it is composed of 4-6 layers of  $\sim 0.1-0.5\mu\text{m}$  cells with  $\Psi \approx 35^\circ$  [72, 73]. A crystal may rotate into an orientation where originally secondary slip becomes highly stressed; this may cause bands of duplex slip.

**3-DBTB.** In single crystals oriented for multiple slip ( $20^\circ\text{C}$ ), parallel bands develop with alternation of the two favored systems [68, 70]. Such behavior is generally found along the  $\langle 111 \rangle \langle 110 \rangle$  zone. In channel angle straining of single crystals, some orientations are stable but some unstable ones break up into small parallelepipeds, (bounded by TB) along the zero strain axis.

**4-DBTB.** In single crystals at high  $T$  notably in torsion, a low density of HAB have developed and thought to be TB much as in 2,3-DBTB [58, 71, 74]. They have been primarily identified by selected area diffraction SAD in TEM. They differ from TB at  $20^\circ\text{C}$  in that they are narrow and compact, that is not layered [74, 77-79]. In Al their development did not lead to dDRX [74, 76-78]; in Cu and Ni, DRX from a single nucleus is followed by multiple twinning (7-DRX).

**5-DBTB.** In polycrystals, the parallelogram bands start to develop at low strains, often resulting in additional parallel bands with alternating slip system (Figure 1d); there may be bands at other angles with still other slip systems. The bands with differing systems give rise to different components of the deformation texture [31, 32, 38, 67-70, 80].

**6-DBTB.** To maintain plastic stability, grains in polycrystals must slip on 5 systems as deduced by Taylor. By slipping in bands with  $\sim 2$  systems, the strain energy is minimized [12, 13, 27, 30-33, 38, 67, 70, 80-85]. Each group of bands slipping

similarly have similar Taylor factors relative to a single crystal and rotate into the same texture component independent of  $T$  [81]. The frequency and location of bands depends on grain orientation, size and orientation of neighbours; it decreases as  $T$  rises due to less constraints such as non-octahedral glide [77-79].

**7-DBTB.** Since the bands are usually transverse to the elongation direction, they rotate into and elongate in the tensile strain direction. At high strains, TB appear as layer boundaries indistinguishable from GB [12, 13, 31-33, 38, 39, 81].

**8-DBTB.** In hot worked polycrystalline Al, deformation bands have been noted at low strains ( $\sim 0.5$ ) by means of POM. This has been confirmed by OIM in which the appearance is similar but with the assurance of a step up in angle followed by an equal step down (Part 2) [82-85]. They have not been easily confirmed by TEM because of similarity to GB and limited field of view. In Fe-25Cr, at  $900^\circ\text{C}$   $\varepsilon = 4$ , TB (MAB-HAB) have been observed because the GB were distinguished by carbide decoration [86] (also noted in thin  $\alpha$ -phase matrix of duplex stainless [66]). In Al 99.7 at  $400^\circ\text{C}$   $0.1\text{s}^{-1}$  to  $\varepsilon = 20-60$ , TB were identified as MAB layer bands by scanning TEM (Kikuchi patterns) [39].

## GRAIN BOUNDARIES AND SGB; SERRATIONS: {-SERV= (SERRATION + DRV)}

**1-SERV.** As strain proceeds in steady state the grain boundaries become serrated (dentillated) as observed in Al alloys (Figures 1, 3 [94]), ferritic steels, copper, nickel, stainless steels and Mg alloys. It arises because the GB migrate to absorb SGB, being limited by balancing surface energy. The half wavelength of the serrations is approximately the subgrain size ( $d_s$  or  $w_s$ ) [34, 35, 39, 57, 80, 81, 87-96]. In the lower SFE metals, the serrations become stronger and give rise to necklace nucleation of DRX as explained later (4-DRX).

**2-SERV.** As strain rises with the subgrains remaining constant in size and equiaxed (7-DRV), the serrations sustain the same dimensions as in 1-SERV [87]. The GB intersections with SGB rearrange as the SGB undergo repolygonization as has been observed over strains up to 60 [12, 13, 39, 88, 94]. With rising  $\epsilon$ , TB becomes more like GB in  $\Psi$  and in alignment. They also become serrated making their distinction ever more difficult [83-85]. At high strains the GB and TB form a layered structure and have been distinguished by STEM [39].

**3-SERV.** At medium strains in Al-5Mg or Al-5Mg-Mn, the GB serrations appear to be based on the initial thick, layered subboundaries [55] (9-DRV) so that they become much more billowy or meandering than in Al [14, 30, 34, 35, 40, 55, 57, 90, 97-99]. Some such billows pinch off, giving the appearance of new grains; however they are found to contain a substructure of similar dimensions to the neighboring grains so they are not nuclei that grow. As the initial grains elongate, they are difficult to distinguish from the new serrations. It is clear that dDRX does not take place in single-phase alloys up to 5.5% Mg; however, particle stimulated nucleation may occur in alloys with large  $Al_6Mn$  particles in which further growth is restricted by fine particles.

**4-SERV.** In the simple two-dimensional view, the subgrains adjacent to GB or TB have two facets that are HAB out of approximately 6. As the grains thin down, more and more subgrains come into contact with the GB and TB so that the fraction of LAB declines and that of HAB

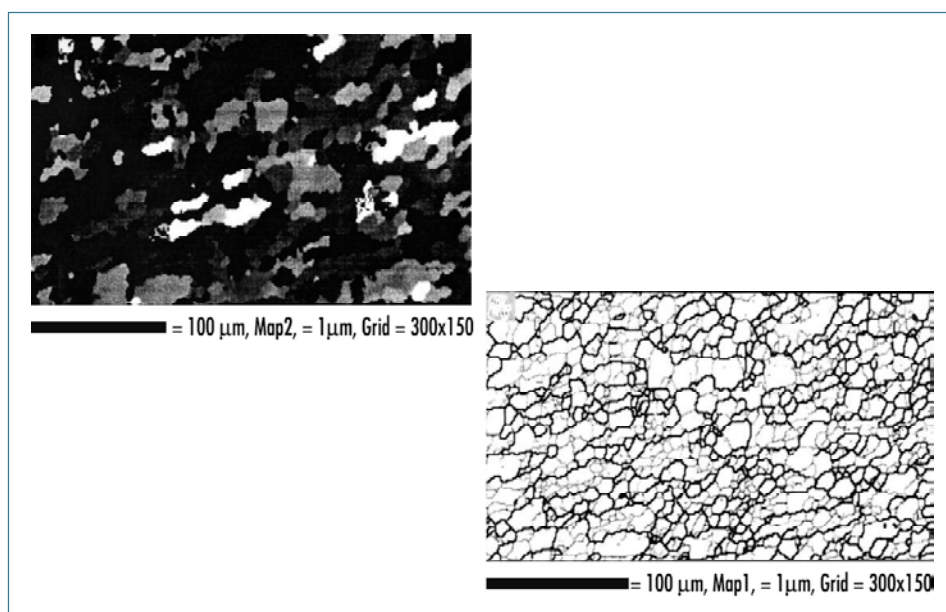


Fig. 3: Scanning electron microscopy of Al-0.48Mg-0.43Si (6060) after torsion to  $\epsilon = 20$  at 400°C, 0.1 s<sup>-1</sup>: a) EBSI, subgrains visible in grains shortened by gDRV, and b) OIM with HAB thick and LAB, SGB faint dashed.

rises [31-33, 39, 58]. This has been confirmed in OIM with little change in the MAB fraction that would arise if SGB were simply accumulating dislocations to rise in  $\Psi$  [83-85]. In a thought experiment on Al undergoing a strain increment of 50% for large equiaxed grains 40 times the subgrain size, the SGB-HAB fraction rises from less than 1% to more than 20%; the introduction of two TB per grain would raise the fraction to about 30% [32].

**5-SERV.** As the GB migrates to absorb SGB lowering energy, there is a small net migration into the grain with the lower spacing of SGB. Such grains have a higher Taylor factor as a result of orientation or texture [39,82,100-104]. The associated evolution of texture has been confirmed by both micro (STEM) and macro texture (XRD) at strains from 10 to 60 (time ~100s) [39].

**6-SERV.** The geometric process of grain pinching-off shortens the grains; such development of refined grains containing substructure (without any nucleation) was called geometric gDRV. The pinching-off leaves the two adjoining grains thicker thus leading to no net decrease in thickness as elongation continues. Furthermore, the sharp ends of pancaked grains pinch off more quickly leading to migration of the triple junction with net thickening. [30-33, 39, 82, 90, 91]. An equilibrium in

grain shape is developed as the thickened regions undergo plastic elongation; a more suitable name is grain dividing gDRV [12, 13, 58, 85, 105, 106]. The mechanism is therefore self-perpetuating leading to a stable structure in which the subgrains maintain the size with 50-70% LAB (50-30%HAB). While the HAB continue to eliminate each other (countering grain thinning), the SGB continue to rearrange in repolygonization. The final cell size equals  $d_s$  and the stress remains at  $\sigma_s$  characteristic of the T and  $\dot{\epsilon}$ ; the subgrain size defines the minimum grain thickness thus grain defining gDRV [12, 13, 58, 105, 106].

**7-SERV.** When an equiaxed equilibrium structure as described in 6-SERV is subjected to a reduction in  $\dot{\epsilon}$ , the substructure will reorganize rapidly through dislocation annihilation (3, 4, 5-DRV) to a large  $d_s$  as described in 8-DRV [107,108]. Because of different grain orientations the rapid enlargement in spacings of SGB in one grain causes the GB to migrate into neighboring grains with smaller spacings. The next result is an increase in grain size thus grain-defining gDRV without any nucleation and growth as in dDRX (4-DRX). This occurs in the nugget of friction stir welds when metal intensely deformed by the pin is deposited behind it.

## DYNAMIC RECRYSTALLIZATION (DRX): {-DRX}

This section deals with classic discontinuous (dDRX) that occurs by nucleation and growth of new grains in low SFE metals primarily alloys of Cu, Ni and  $\gamma$ Fe, notably stainless steels where the substructure is preserved; single-phase polycrystals are described unless otherwise stated [1-6, 9, 15, 17]. The word classic indicates that the starting material is in a strain free condition and the substructure has undergone DRV at same  $T_D$  and  $\dot{\epsilon}$  as DRX. There will be explanations of pseudo dDRX, geometric gDRX, continuous cDRX (both multi and single phase) and particle-stimulated nucleation PSN-DRX [12, 13, 58, 109-113].

**1-DRX.** The transient starts with a DRV substructure that for a given  $\dot{\epsilon}$  and homologous  $T$  is less polygonized than in high SFE Al or  $\alpha$ -Fe [112]; after a common strain during holding at  $T_D$ , the time for SRX decreases markedly as SFE decreases [6, 22, 112, 114]. Nucleation occurs before steady state from DRV reducing strain hardening. Such behavior is found in Al and  $\alpha$ -Fe with impurities less than 100ppm [115-119].

**2-DRX.** The critical strain  $\epsilon_C$  for DRX is always higher than that for SRX indicative that the concurrent straining injects new dislocations into potential nuclei that would ripen through SRV at  $\dot{\epsilon} = 0$  [4, 5, 15, 17, 120-125]. This is confirmed by nucleation at lower  $\epsilon_C$  if  $\dot{\epsilon}$  is reduced either suddenly or in stress relaxation [126]; these are cases of pseudo dDRX. In polycrystals, nucleation is generally associated with preceding formation of marked GB serrations [80, 120-124]. If  $\dot{\epsilon}_C$  is high (low  $T$ , high  $\epsilon$ ), nuclei may be associated with TB [124, 125]; in single crystals nucleation is always at TB (7-DRX).

**3-DRX.** A peak develops in the flow curve at 30-40% DRX and flow softening takes place until the first wave of DRX is completed and a steady state is attained with a grain size  $D_S$  [15, 17, 120, 121]. DRV substructure develops in the new grains as straining continues after their nucleation [124-127].

**4-DRX.** The early nuclei form a necklace along the initial GB and stop growing at a size and additional  $\epsilon$  ( $= \epsilon \times \text{time}$ ) as a result of the newly inserted dislocations that

reduce GB mobility [17, 120, 128, 129]. Additional necklaces nucleate and stop at the common size,  $D_S$  that is dependent on stress or  $Z$  in similar manner as expressed in Equations 1 and 2.

**5-DRX.** At low  $\dot{\epsilon}$ ,  $Z$ , high  $T$  or fine initial grain size  $D_i$  where  $D_S$  would be larger than  $D_i/2$ , the flow curve exhibits multiple peaks that reduce in scale until steady state is reached; the cycles indicate multiple partial waves of DRX that gradually increase the grain size [124, 125, 130]. At fixed  $T_D$  and  $\dot{\epsilon}$ , multiple peaks can be produced by decreasing the initial grain size.

**6-DRX.** In steady state, substructure starts being replaced as soon as grains start to grow. Nucleation occurs fairly randomly at boundaries of oldest grain clusters [120, 124]. The equilibrium size  $D_S$  is dependent on  $\sigma_S$  or  $Z$  as in Equations 1 and 2 with altered constants ( $p \sim 0.8$ ).

**7-DRX.** In a single crystal, the flow curve rises to much higher  $\epsilon_{CX}$  and stress above  $\sigma_p$  for a given  $Z$  condition [131-134]. Generally only one nucleus forms and grows very rapidly due to the high dislocation density by means of multiple twinning to develop very mobile GB. The flow stress drops drastically and then continues at the  $\sigma_S$ ,  $D_S$  and  $d_S$  as defined by that  $Z$  in polycrystals.

**8-DRX.** The constitutive equations in 2-DRV may be applied to either the peak stress  $\sigma_p$  ( $Q_{HWP}$ ) to  $\sigma_S$  ( $Q_{HWS}$ ) with constants dependent on material (both higher than  $Q_D$  diffusion) [10,15]. In  $\gamma$  stainless steels  $Q_{HWP}$  rises uniformly with total metallic solute content [10, 135].

**9-DRX.** The average subgrain size  $d_s$  in steady state with DRX in combination with  $d_{ec}$  just before nucleation obey the equations in 2-DRV [127]. In consequence one can say that  $d_s$  controls the flow stress as in simple DRV (Equations 3, 4). For same  $\sigma_S$  (somewhat equivalent conditions),  $d_s$  in  $\gamma$  stainless is smaller by a factor 0.7 than in Al alloys [36].

**10-DRX.** In some similarity to 8-DRV there is a transient to characteristic  $\sigma_S$ ,  $d_s$  and  $D_S$  when there is a change  $\Delta\epsilon$  or  $\Delta T$ . The

transient involves a single peak or multiple peaks according to the grain sizes (5-DRX) [130]. Because of the different partial substructures, the transients in these pseudo DRX are likely to differ from those in classic DRX to the same final  $\epsilon$ . Pseudo DRX has been induced in Al only by  $\Delta\epsilon$  factors of  $10^3$  or  $10^4$  whereas  $\Delta\epsilon$  factors of  $10^1$  or  $10^2$  simply caused an increase in  $d_s$  (8-DRV) [54].

**11-DRX.** Notably in HCP Mg alloys, subgrains develop near GB and along twin boundaries due to slip on several systems while the grain centers are mainly restricted to basal glide [95, 96, 136, 137]. The GB and twin boundaries develop serrations and dDRX forms several layers of new grains (size defined by  $T$ ,  $\dot{\epsilon}$ ,  $Z$  as in 4,9-DRX) that do not spread into the grain centers. The refined mantle undergoes repeated dDRX as in steady state (6,9-DRX). Deformation proceeds mainly in the GB mantle (somewhat like shear bands); this phenomenon has been called core/mantle or rotation DRX.

**12-DRX.** In alloys with large hard second phase, strain concentrates in regions around the particles. The finer substructure with higher  $\Psi$  walls give rise to particle stimulated nucleation (PSN) of new grains classed as PSN-SRX or PSN-DRX [57,138-140]. PSN-SRX occurs in both Al-Mn and Al-Mg-Mn alloys due to  $Al_6Mn$  but PSN-DRX is found only in Al-Mg-Mn where Mg reduces the level of DRV [140]. In as-cast  $\gamma$  stainless steels, segregated  $\alpha$  stringers increase peak stress but reduce peak strain as DRX grains form near interphase boundaries but only in the  $\gamma$  grains [120, 121].

**13-DRX.** Continuous SRX occurs in heavily cold worked two phase alloys in which many cell boundaries have been altered to HAB due to particle pinning. The cell walls undergo changes in character to true GB [141]. In straining under superplastic conditions  $\sim 10^3$  (after subjection to an intense TMP) alloys of Al-Cu-Mg and Al-Li-Mg-Cu with added dispersoid develop fine grains through cDRX at a much faster rate than in simple annealing at same  $T$  [141-146].

**14-DRX.** On the basis of increase in fraction of HAB, cDRX has been postulated

in single phase Al on the theory that all SGB march upwards in  $\Psi$  with strain [94, 146, 147]. This theory has been countered by geometric DRX (15-DRX) or grain defining DRV (6,7-SERV) [33, 39, 58, 94]. cDRX has also been postulated in  $\gamma$ -stainless steels during the transient before  $\varepsilon_C$  as an

explanation of the rise of HAB on cells that have not yet nucleated. In  $\alpha$ -stainless it has been postulated during warm working (11-DRV) where subgrain size has increased but  $\Psi$  has not decreased [148].

**15-DRX.** Geometric gDRX was the name given to the phenomenon in 6-SERV. The

formation of small grains from pinched-off pancaked grains and the presence of a substructure within them had the appearance of DRX purely from geometry [33, 39]. Grain dividing or defining gDRV avoids confusion [12, 13, 58].

## SUMMARY

The DRV substructure developments {DRV}, that depend on dislocation glide, climb, combination and stress fields have been described in discrete steps related to rising strain. The formation of deformation bands with intervening TB {DBTB}, that are required for plastic stability in slipping polycrystals, forces dislocations into a different organization from the DRV substructure, leading to high misorientation. When grain thickness approaches  $d_S$  {SERV}, the interaction of SGB and GB induce serrations and net migrations that rearrange the grain structure in gDRV. Finally the section on DRX provides clear distinction from DRV that was also clarified by the contrast. In Part II [Metallurgical Science and Technology Vol. 28-2], the evidence will be critically examined to show where various techniques have limitations that cause confusion. In Part II, the experimental techniques will be analyzed to find consistent evidence and to undo the limitations of each. By judicious consideration of mutually supportive findings, a non-conflicting mosaic can be developed.

Table of Symbols and Acronyms

a, b, c, e,	Materials constant
A, A', A''	Material constants
b	Burgers vector
BW	Block walls
cDRX	Continuous dynamic recrystallization
D	Grain size
DB	Deformation Band
DBTB	Deformation Band-Transition Boundary
cDRX	Continuous DRX
dDRX	Discontinuous DRX
$D_i$	Initial grain size
$D_0$	Diffusion constant
DRV	Dynamic recovery
DRX	Dynamic recrystallization
$d_s$	Steady state subgrain size
$D_s$	Steady state grain size
$f_n$	Function of $\sigma_s$ , eqn. (4)
G	Shear elastic modulus
GB	Grain boundary
gDRV	Grain defining DRV
gDRX	Geometric DRX
GNB	Geometrical necessary boundary
HAB	High angle boundary
$k_B$	Boltzman constant
LAB	Low angle boundary
MAB	Mediun angle boundary
n	Stress exponent, sinh law equation
n'	Stress exponent, power law equation
OIM	Orientation image microscopy
p	$d_s$ exponent, eqn. (2)
PSN	Particle stimulated nucleation
PSN-DRX	PSN of dynamic recrystallization
PSN-SRX	PSN of static recrystallization

Q	Activation energy
$Q_{CR}$	Q for creep
$Q_D$	Q lattice diffusion
$Q_{HW}$	Q for hot working
$Q_{HWP}$	Q for hot working at peak
$Q_{HWS}$	Q for hot working at steady state
R	Gas constant
sinh	Hyperbolic sine, eqn. (4)
SAD	Selected area diffraction
SERV	Serration + DRV Section
SFE	Stacking fault energy
SGB	Subgrain boundaries
SIB	Strain induced boundaries
SRV	Static recovery
SRX	Static recrystallization
STEM	Scanning transmission electron microscopy
$S_w$	Dislocation spacing in subgrain walls (see 3-DRV)
T	Temperature
$T/T_M$	Homologous T, $T_M$ melting T(K)
TB	Transition boundaries
TD	Deformation temperature
TEM	Transmission electron microscopy
$w_s$	Wall spacing
w-DRV	Warm DRV
Z	Zener-Hollomon parameter
$\alpha$	Stress multiplier, sinh eqn. (4)
$\alpha_{Fe}$	Ferrite
$\beta$	Stress multiplier, exponential law eqn. (4)
$\gamma_{Fe}$	Austenite
$\varepsilon$	Strain
$\varepsilon_{CX}$	Critical strain for DRX
$\dot{\varepsilon}$	Strain rate

$\epsilon_S$	Stationary strain rate
$\epsilon_F$	Ductility as strain to fracture
$\theta$	Strain hardening rate
$\Psi$	Misorientation angle
$\Psi_S$	$\Psi$ at steady-state
$\rho_i$	Dislocation density in subgrains
$\sigma$	Stress
$\sigma_P$	Peak stress
$\sigma_S$	Steady-state stress

## REFERENCES

- [1] H.J. McQueen, Encyclopedia of Materials Science and Technology, Elsevier Science, Oxford, UK. 2001, pp. 2375-2381.
- [2] J.J. Jonas, C.M. Sellars and W.J. McG. Tegart, Metall. Rev., Vol. 14, 1969, 1.
- [3] C.M. Sellars, W.J. McG. Tegart, Int. Met. Rev., Vol. 17, 1972, 1.
- [4] H.J. McQueen and J.J. Jonas, Treatise on Materials Science and Technology, Vol. 6, Plastic Deformation of Materials, New York, 1975, Academic Press, pp. 393-493.
- [5] H. Mecking and G. Gottstein, Recrystallization of Metallic Materials, F. Haessner, Ed., Dr. Reidereer Verlag Stuttgart, 1977, pp. 195-212.
- [6] H.J. McQueen and D.L. Bourell, Inter-relationship of Metal. Structure and Formability, A.K.Sachdev, J.D. Embury, eds., Met. Soc., AIME, Warrendale, PA 1987, pp. 341-368; J. Met., Vol. 39 [9], 1987, pp. 28-35.
- [7] H.J. McQueen, E. Evangelista and M.E. Kassner, Z. Metallkde., 82 (1991), pp. 336-345.
- [8] H.J. McQueen, Advances in Metallurgy of Aluminum Alloys, (J.T. Staley Symp.), M. Tiryakioğlu, Ed., ASM Intl., Materials Park, OH. (2001), pp. 351-360.
- [9] H.J. McQueen, (ICSMA 13, Budapest), T. Ungar, et al., Eds., Mat. Sci. Eng., A387-389 (2004), pp. 203-208.
- [10] H.J. McQueen and N.D. Ryan, Mat. Sci. Eng., A322 (2002), pp. 43-63.
- [11] H.J. McQueen, Metal. Mat. Trans., 33A (2002), pp. 345-362.
- [12] H.J. McQueen and S. Spigarelli, Mat. Sci. Eng., A462 (2007), pp. 37-44.
- [13] H.J. McQueen, E. Evangelista, M. Cabbibo and G. Avramovic-Cingara, Can. Metal Quart. 47 (2008), 71-82.
- [14] H.J. McQueen, W. Blum, Aluminium 80, [10], (2004), pp. 1151-1159; pp. 1263-1270; pp. 1347-1355.
- [15] N.D. Ryan and H.J. McQueen, J. Mat. Proc. Tech., 21 (1990), pp. 177-199.
- [16] H.J. McQueen, Mat. Sci. Eng., A101 (1987), pp. 149-160.
- [17] H.J. McQueen and W.B. Hutchinson, Deformation of Polycrystals, N. Hansen et al., Eds., Riso Natl. Lab., Roskilde, DK. (1981), pp. 335-342.
- [18] J. Hausselt and W. Blum, Acta Met., 24 (1976), pp. 1027-1039.
- [19] T. Hasegawa, T. Yakou and U.F. Kocks, Acta Met., 30 (1982), pp. 235-243.
- [20] H.J. McQueen and S. F olup, Forging and Properties of Aerospace Materials, Metals Society, London, (1978), pp. 164-169.
- [21] Hsun Hu, Recovery and Recrystallization of Metals, Gordon and Breach, New York (1963), pp. 311-364.
- [22] H.J. McQueen, Trans. Japan Inst. Met., 9 Suppl. (1968), pp. 170-77.
- [23] F. Garofalo, Fundamentals of Creep and Rupture in Metals, Macmillan, New York, 1965.
- [24] H.J. McQueen, W.A. Wong and J.J. Jonas, Can. J. Phys., 45 (1967), pp. 1225-34.
- [25] H.J. McQueen, J.E. Hockett, Met. Trans., 1 (1970), pp. 2997-3004.
- [26] H.J. McQueen, J.K. Solberg, N. Ryum and E. Nes, Phil. Mag., 60 (1989), pp. 473-485.
- [27] T. Sheppard, Met. Tech., 8 (1981), pp. 130-141.
- [28] S.V. Raj and G.M. Pharr, Mat. Sci. Eng., 81 (1986), pp. 217-237.
- [29] D.J. Abson and J.J. Jonas, Met. Sci., 4 (1970), pp. 24-28.
- [30] W. Blum and H.J. McQueen, Aluminum Alloys Physical and Mechanical Properties, ICAA5, J.H. Driver, et al., Mat. Sci. Forum, (1996), pp. 31-42; pp. 217-222.
- [31] H.J. McQueen and W. Blum, Recrystallization and Related Topics., Rex '96, T.R. McNelley, ed., Monterey Inst. Advanced Studies, CA. (1997), pp. 123-136.
- [32] H.J. McQueen and W. Blum, Al Alloys Physical and Mechanical Properties, (ICAA6), T. Sato, ed., Japan Inst. Metals (1998), pp. 99-112.
- [33] H.J. McQueen, W. Blum, Mat. Sci. Eng., A290 (2000), pp. 95-107.
- [34] H.J. McQueen, W. Blum, Q. Zhu and V. Demuth, Advances in Hot Deformation, T.R. Bieler and J.J. Jonas, eds., TMS-AIME, Warrendale, PA. (1994), pp. 253-250.
- [35] W. Blum, Q. Zhu, R. Merkel and H.J. McQueen, Z. Metallkde, 87 (1996), pp. 14-23.
- [36] W. Straub and W. Blum, Hot Workability of Steels and Light Alloys-Composites, H.J. McQueen, E.V.Konopleva, N.D. Ryan, eds., Met. Soc. CIM, Montreal (1996), pp.189-204.
- [37] W. Blum, The Johannes Weertman, Symposium, R.W. Arsenault, et al., eds., TMS-AIME, Warrendale, PA. (1996), pp. 103-117.
- [38] R.D. Doherty, D.A. Hughes, F.J. Humphreys, J.J. Jonas, D. Juul-Jansen, M.E. Kassner, W.E. King, T.R. McNelley, H.J. McQueen and A.D Rollett, Mat. Sci. Eng., 238 (1998), pp. 219-274.

- [39] J.K. Solberg, H.J. McQueen, N. Ryum and E. Nes, *Phil. Mag.*, 60 (1989), pp. 447-471.
- [40] G.A. Henshall, M.E. Kassner and H.J. McQueen, *Metal. Trans.*, 23A (1992), pp. 881-889.
- [41] M.E. Kassner and M.E. McMahon, *Met. Trans.*, 18A (1987), pp. 835-846.
- [42] A.K. Mukherjee, *Treatise on Mat. Sci. and Tech.*, R. J. Arsenault, Academic, N.Y., 6 (1975), pp. 164-224.
- [43] D. Kuhlman-Wilsdorf, *Work Hardening in Tension and Fatigue*, A.W. Thompson, ed., AIME, Warrendale, PA. (1977), pp. 1-44.
- [44] A. Orlova and J. Cadek, *Mater. Sci. Eng.*, 81 (1986), pp. 371-377.
- [45] D. Caillard and J.L. Martin, *Rev. Phys. Appl.*, 22 (1987), pp. 169-183.
- [46] W. Blum and H. Schmidt, *Res. Mech.* 9 (1983), p. 105.
- [47] W. Blum and A. Finkel, *Acta Met.*, 30 (1982), pp. 1705-1715.
- [48] V.K. Lindroos, H.M. Miekko, *Phil. Mag.*, 16 (1967), 593-610; 17 (1968), pp. 119-33.
- [49] H.J. McQueen and M.E. Kassner, *Mat. Sci. Eng.*, A410-411 (2005), pp. 58-61.
- [50] H.J. McQueen and M.E. Kassner, *Superplasticity in Aerospace*, T.R. McNelley and H.C. Heikkinen, eds., TMS-AIME (1988), pp. 77-96.
- [51] W. Blum, *Scripta Met.*, 16 (1982), pp. 1353-1357.
- [52] H.J. McQueen, G. Avramovic-Cingara, A. Salama and T.R. McNelley, *Scripta Met.*, 23 (1989), pp. 273-278.
- [53] I. Ferreira and R.G. Stang, *Acta Met.* 31 (1983), p. 585.
- [54] Y. Huang and F.J. Humphreys, *Acta Mater.*, 45 (1997), pp. 4491-4503.
- [55] I. Poschmann and H.J. McQueen, *Physica Status Solidi*, 149 (1995), pp. 341-348.
- [56] H.J. McQueen and O.C. Celliers, *Can. Metal. Quart.*, 35 (1996), pp. 305-319; 36 (1997), pp. 73-86.
- [57] W. Blum, Q. Zhu, R. Merkel and H.J. McQueen, *Mat. Sci. Eng.*, A205 (1996), pp. 23-30.
- [58] H.J. McQueen and M.E. Kassner, *Scripta Mater.*, 51 (2004), pp. 461-465.
- [59] D.A. Hughes, Q. Liu, D.C. Chrzan and N. Hansen, *Acta Mater.*, 45 (1997), pp. 105-112.
- [60] B. Bay, N. Hansen, D.A. Hughes and D. Kuhlmann-Wilsdorf, *Acta Metal. Mat.*, 40 (1992), pp. 205-219.
- [61] D.A. Hughes and N. Hansen, *Advances in Hot Deformation Textures and Microstructures*, J.J. Jonas, et al. eds. TMS-AIME, Warrendale, PA. (1995), pp. 427-444.
- [62] D.A. Hughes and A. Godfrey, *Hot Deformation of Al Alloys II*, T.R. Bieler, et al., eds. TMS, AIME, Warrendale, PA. (1998), pp. 23-36.
- [63] N. Hansen and D. Juul-Jensen, *Hot Working of Al Alloys*, T.G. Langdon, et al., eds. TMS AIME, Warrendale, PA. (1991), pp. 3-20.
- [64] W. Pantleon (ICSMA 13), *Mat. Sci. Eng.*, A387-389 (2004).
- [65] W. Pantleon (IPSMA 10), *Mat. Sci. Eng.*, A462 (2006).
- [66] P. Cizek and B.P. Wynne, *Mat. Sci. Eng.*, A230 (1997), pp. 88-94.
- [67] C.S. Barrett, L.H. Levenson, *Trans. AIME*, 137 (1990), pp. 112-127.
- [68] D. Kuhlman-Wilsdorf, *Acta Mater.*, 47 (1999), pp. 1697-1712.
- [69] J. Gil-Sevilano, P. van Houtte and E. Aernoudt, *Prog. Mat. Sci.*, 25 (1980), p. 69.
- [70] B. Jaoul, *Étude de la Plasticité et Application aux Métaux*, Dunod, Paris, 1965.
- [71] G.Y. Chin, *Inhomogeneity Plastic Deformation*, ASM, Metals Park, OH (1973), pp. 83-112.
- [72] P.J. Wilbrandt, P. Haasen, *Z. Metall.*, 71 (1980), pp. 273-278, pp. 385-395.
- [73] A. Berger, P.J. Wilbrandt, P. Haasen, *Acta Metall.*, 31 (1983), pp. 1433-1443.
- [74] M.E. Kassner, *Metal. Trans.*, 20A (1989), pp. 2182-2185.
- [75] C.S. Lee, B.J. Duggan, *Acta Metal. Mater.*, 41 (1993), pp. 2691-2699.
- [76] M. Richert, H.J. McQueen and J. Richert, *Can. Metal. Quart.*, 37 (1998), pp. 449-457.
- [77] C.L. Maurice, M.C. Theysier and J.H. Driver, *Advances in Hot Deformation Textures and Microstructures*, J.J. Jonas, et al., eds., TMS-AIME, Warrendale, PA. (1995), pp. 411-425.
- [78] J.H. Driver, *Microstructural and Crystallographic Aspects of Recrystallization*, N. Hansen, et al. Eds., Riso Natl. Lab, Roskilde, DK. (1995), pp. 25-36.
- [79] M.C. Theysier, B. Chenal, J.H. Driver, N. Hansen, *Phys. Stat. Sol.*, A149 (1995), pp. 367-378.
- [80] F.N. Rhines, *Inhomogeneity of Plastic Deformation*, ASM Metals Park, OH (1973), pp. 251-284.
- [81] H.J. McQueen and H. Mecking, *Z. Metallkunde*, 78, (1987), pp. 387-395.
- [82] H.J. McQueen, *Proc. ICOTOM 12*, J.A. Szpunar, ed., NRC Res. Pub., Ottawa (1999), pp. 836-841.
- [83] G. Avramovic-Cingara, H.J. McQueen and D.D. Perovic, *Light Metals/Métaux Legers 2004*, D. Gallienne, R. Ghomaschi eds., Met. Soc., CIM, Montreal (2004), pp. 141-152.
- [84] G. Avramovic-Cingara and H.J. McQueen, (ICAA10 Vancouver), *Mat. Res. Forum*, 519-523 (2006), pp. 1659-1664.
- [85] G. Avramovic-Cingara and H.J. McQueen, *Aerospace Materials Manufacturing (and Repairs)*, Emerging Techniques, M. Jahazi, M. Elboudjani and P. Patnaik, eds. Met. Soc., CIM Montreal, (2006), pp. 173-186.
- [86] R. Lombry, C. Rossard and B. Thomas, *Rev. Met.*, 78 (1981), pp. 975-988.
- [87] H.J. McQueen, N.D. Ryan, E.V. Konopleva and X. Xia, (Engineering Aspects Of Grain Boundary and Interface Science), *Can. Metal. Quart.*, 34 (1995), pp. 219-229.
- [88] O. Knustad, H.J. McQueen, N. Ryum, J.K. Solberg, *Practical Metal.*, 22 (1985), pp. 215-229.
- [89] H.J. McQueen, *Hot Deformation of Aluminum Alloys*, T.G. Langdon and H.D. Merchant, Eds., TMS-AIME, Warrendale, PA. (1991), pp. 31-54.
- [90] H.J. McQueen, E.V. Konopleva, W. Blum, *Microstructural Science*, 22 (1995), pp. 299-314.
- [91] E.V. Konopleva, H.J. McQueen, E. Evangelista, *Mat. Characterization*, 34(1995), pp. 251-264.
- [92] M.M. Myshlyaev, O.N. Senkov, and V.A. Likhachev, *Strength of Metals and Alloys*, ICSMA 7, H.J. McQueen, et al., eds. Pergamon Press, Oxford (1985), pp. 841-846.
- [93] I. Gutierrez and M. Fuentes, *Recrystallization '90*, T. Chandra, ed., TMS-AIME, Warrendale, PA. (1990), pp. 807-812.
- [94] S. Gourdet, C. Chovel and H.J. McQueen, *Aluminum Transactions* 3 (2001), pp. 59-68.
- [95] M.M. Myshlyaev, H.J. McQueen, A. Mwembela and E.V. Konopleva, *Mat. Sci. Eng.*, A337, (2002), pp. 121-133.
- [96] V.M. Khlestov, E.V. Konopleva and H.J. McQueen, *Mat. Sci. Tech* 18, (2002), pp. 54-60.
- [97] E. Cerri, E. Evangelista and H.J. McQueen, *High Temp. Mat. Proc.* 18 (1999), pp. 227-240.
- [98] I. Samajdar, P. Ratchev, B. Verlinden, P. Van Houtte, P. DeSmet, *Mater. Sci. Eng.*, A247 (1998), pp. 58-66.
- [99] F.J. Humphreys and M.R. Drury, *Aluminum Technology*, T. Sheppard, ed., Inst. Metals, London (1986), pp. 191-196.
- [100] S. Gourdet, A. Girinon and F. Montheillet, *Thémec '97*, T. Chandra and T. Sakai, eds., TMS AIME, Warrendale, PA. (1997), pp. 2117-2123.

- [101] H.J. McQueen, W. Blum, S. Straub and M.E. Kassner, *Scripta Metal Mat.*, 28 (1993), pp. 1299-1304.
- [102] N.J. Grant and A.R. Chaudhuri, *Deformation and Fracture at Elevated Temperatures*, N.J. Grant and A.W. Mullendore, eds., MIT Press, MA. (1965), pp. 105-164.
- [103] G.R. Canova, U. Kocks and J.J. Jonas, *Acta Metal.*, 32 (1984), pp. 211-226.
- [104] J. Baczynski and J.J. Jonas, *Metal. Mat. Trans.*, 29A (1998), pp. 447-462.
- [105] T. Pettersen, B. Holmedal and E. Nes, *Metal. Mat. Trans.*, 34A (2003), pp. 2737-2744.
- [106] T. Petterson and E. Nes, *Metal. Trans.* 34A (2003), pp. 2727-2736.
- [107] M. Cabibbo, H.J. McQueen, E. Evangelista, S. Spigarelli, M. Di Paola, A. Falchero, *Mater. Sci. Eng.*, A460-461 (2007), pp. 86-94.
- [108] H.J. McQueen, M. Cabibbo, E. Evangelista, *Mat. Sci. Tech.*, 23 (2007), pp. 803-809.
- [109] H.J. McQueen, (ICAA10), *Mat. Res. Forum*, pp. 519-523, (2006), pp. 1493-1498.
- [110] H.J. McQueen, *Light Metals 2000*, J. Kazadi, et al. eds., Met Soc. CIM, Montreal (2000), pp. 287-296.
- [111] H.J. McQueen, and J.J. Jonas, *Aluminum Alloys '90*, (2nd Int. Conf., Beijing), C.Q. Chen, ed. (1990), pp. 727-742.
- [112] H.J. McQueen, *Thermomechanical Processing of Steel* (Jonas Symposium), S. Yue, E. Essadiqi eds., Met. Soc. CIM, Montreal (2000) pp. 323-333.
- [113] H.J. McQueen, *Aluminum Alloys, Physical Mechanical Properties*, ICAA9, J.F. Nie, et al., eds., Monash Univ., Melbourne, Australia (2004), pp. 351-356.
- [114] L. Gavard, M. Montheillet and H.J. McQueen, *Proc. ICOTOM 12*, J.A. Szpunar, ed., NRC Res. Pub., Ottawa (1999), pp. 878-883.
- [115] D. Ponge, M. Bredehoff and G. Gottstein, *Scripta Metal.*, 37 (1997), pp. 1769-1775.
- [116] H. Yamagata, *Scripta Metal. Mat.*, 21 (1992), pp. 201-203, pp. 727-732, pp. 1157-1160.
- [117] H. Yamagata, *Scripta Metal. Mat.*, 23 (1994), pp. 411-416.
- [118] M.E. Kassner, H.J. McQueen, J. Polard, E. Evangelista and E. Cerri, *Scripta Metal. Mat.*, 1 (1994), pp. 1331-1336.
- [119] G. Glover, C.M. Sellars, *Metall. Trans.*, 3 (1972), 2271; 4 (1973), pp. 765.
- [120] H.J. McQueen, E. Evangelista and N.D. Ryan, *Recrystallization ('90) in Metals and Materials*, T. Chandra, ed., TMS-AIME, Warrendale, PA. (1990), pp. 89-100.
- [121] E. Evangelista, N.D. Ryan and H.J. McQueen, *Metal Sci. Tech.*, 1987, 5, (2), pp. 50-58.
- [122] H.J. McQueen, Y. Cui, B. Li, Q. Meng, N.D. Ryan, *Strip Casting, Hot/Cold Working of Stainless Steels*, Met. Soc., CIMM, Montreal, (1993), pp. 181-192.
- [123] X. Xia, H.J. McQueen, N.D. Ryan, B. Li, Q. Meng and Y. Cui, *ibid* 122, (1993), pp. 117-129.
- [124] H.J. McQueen and P. Sakaris, *Aluminum Alloys, Physical Mechanical Properties*, L. Arnberg, et al., eds., NTH-Sinteff, Trondheim, Norway, (1992), 2, pp. 179-184.
- [125] L. Blaz, T. Sakai and J.J. Jonas, *Met. Sci.*, 17 (1983), pp. 609-616.
- [126] H.J. McQueen, L. Vazquez, *Mater. Sci. Eng.*, 81 (1986), pp. 355-369.
- [127] L. Fritzmeier, M. Luton and H.J. McQueen, *Strength of Metals and Alloys*, P. Haasen, et al., eds., Pergamon Press, Frankfurt (1979), pp. 95-100.
- [128] C.M. Sellars, *Phil. Trans. Roy. Soc.*, A288 (1978), pp. 147-158.
- [129] M. Winning, *Recrystallization and Grain Growth 2001*, G. Gottstein and D.A. Molodov, Springer-Verlag, pp. 21-38; pp. 193-204.
- [130] T. Sakai and J.J. Jonas, *Acta Metall.*, 32 (1984), pp. 189-209.
- [131] H.J. McQueen and N. Ryum, *Scand. J. Met.* 14 (1985), 183-194.
- [132] G. Gottstein, S. Deshpande, *Mater. Sci. and Eng.*, 94 (1987), 147.
- [133] G. Gottstein, *Met. Sci.*, 17 (1983), 497-502.
- [134] P. Karduck, G. Gottstein and H. Mecking, *Acta Metal.*, 31 (1983), pp. 1525-1536.
- [135] N.D. Ryan, H.J. McQueen, *Stainless Steels '87*, Inst. Metals, London (1988), pp. 498-507.
- [136] S.E. Ion, F.J. Humphreys and S.H. White, *Acta Metal.*, 30 (1982), pp. 1909-1919.
- [137] F.J. Humphreys, *Deformation of Polycrystals*, N. Hansen, et al., eds., RISO Natl. Lab., Roskilde, Denmark (1981), pp. 305-310.
- [138] H.J. McQueen, E. Evangelista, J. Bowles and G. Crawford, *Met. Sci.*, 18 (1984), pp. 395-402.
- [139] E. Evangelista, H.J. McQueen, E. Bonetti, *Deformation of Multi-Phase and Particle Containing Materials*, J. Bilde-Sorenson, et al., eds., Riso Natl. Lab., Roskilde, DK (1983), pp. 243-250.
- [140] F.J. Humphreys and P. Kalu, *Acta Metal.* 35 (1987), pp. 2815-2829.
- [141] H. Ahlborn, E. Hornbogen and U. Koster, *J. Mat. Sci.*, 4 (1969), pp. 944-950.
- [142] R. Grimes, M.J. Stowell and B.M. Watts, *Metals Tech.*, 3 (1976), pp. 154-180.
- [143] B.M. Watts, M.J. Stowell, B.L. Baikie, D.G. Owen, *Met. Sci.*, 10 (1976), pp. 189-197, pp. 198-205.
- [144] S.J. Hales, T.R. McNelley and H.J. McQueen, *Metal. Trans.*, 22A (1991), pp. 1037-1047.
- [145] G. Avramovic-Cingara, K.T. Aust, D.D. Perovic, G. Palumbo and H.J. McQueen, *Can. Metal. Quart.*, 34 (1995), pp. 265-273.
- [146] S. Gourdet and F. Montheillet, *Mat. Sci. Eng.*, A283 (2000), pp. 274-288.
- [147] S. Gourdet and M. Montheillet, *Acta Mater.*, 51 (2003), pp. 2685-2699.
- [148] A.N. Belyakov and R.O. Kaibyshev, *Phys. Metal. Metallog.* 78 [1], 1994, pp. 85-90.
- [149] H. Zhang, E.V. Konopleva and H.J. McQueen, (ICSMA12, M.J. Mills, ed.), *Mat. Sci. Eng.*, A319-321, (2002), pp. 711-715.
- [150] G. Avramovic-Cingara, H.J. McQueen, I. Szkrumelak and K. Conrod, *Microstruct. Sc.*, 17, (1989), pp. 375-392.